ELSEVIER

Earth and Planetary Science Letters 195 (2002) 277–290

EPSL

www.elsevier.com/locate/epsl

Experimental evidence for high noble gas solubilities in silicate melts under mantle pressures

Burkhard C. Schmidt *, Hans Keppler [1]

Bayerisches Geoinstitut, Universität Bayreuth, D-95440 Bayreuth, Germany

Received 17 July 2001; received in revised form 1 November 2001; accepted 19 November 2001

Abstract

The solubilities of Ar and Xe in Fe-free synthetic haplogranitic and tholeiitic melts were experimentally determined in the pressure range of 1–11 GPa and at temperatures between 1500 and 2000°C. Experiments were performed in a piston cylinder apparatus (1–3 GPa) and in a multi-anvil apparatus (2–11 GPa). The noble gas concentrations in the quenched glasses were determined with electron microprobe. As a function of pressure, Ar solubility increases linearly up to about 4–5 GPa where it reaches about 4.0 and 0.8 wt% for the haplogranitic and tholeiitic melt, respectively. At higher pressure the amount of dissolved Ar remains constant, suggesting that some threshold concentration is reached. The Xe solubility in tholeiite melt exhibits a very similar pattern. It increases linearly up to about 6 GPa, where a threshold concentration of 0.8 wt% is reached. A further increase of pressure up to 11 GPa does not result in changes in Xe solubility. The leveling off in noble gas solubility at high pressures may imply that the interstitial sites in the melt structure, suitable for the accommodation of noble gas atoms, are fully occupied. Indeed, the experimental data can be successfully reproduced with the Langmuir isotherm, implying a solubility model in which the gas atoms occupy a certain population of interstitial sites. However, the data can be equally well described by a model assuming mixing of the noble gas atoms with the oxygen atoms of the silicate melt. From a thermodynamic point of view, the constant noble gas solubility at high pressures simply implies that the partial molar volumes of the respective noble gas in the fluid and in the melt are equal. Our results differ from those of Chamorro-Perez et al. [Earth Planet. Sci. Lett. 145 (1996) 97–107; Nature 393 (1998) 352–355] who reported an abrupt, order-of-magnitude drop of Ar solubility in silica and olivine melt at around 5 GPa, suggesting that melt densification results in an abrupt decrease of the hole size distribution. A geochemical consequence of our results is that noble gases remain incompatible elements at pressure conditions covering most of the upper mantle. Therefore partial melting remains an efficient process in extracting noble gases and other volatiles from the Earth's mantle.

Keywords: noble gases; solubility; silicate melts; high pressure

* Corresponding author. Tel: +49-921-553726; Fax: +49-921-553769.
E-mail address: burkhard.schmidt@uni-bayreuth.de (B.C. Schmidt).

[1] Present address: Mineralogisches Institut, Universität Tübingen, Wilhelmstr. 56, D-72074 Tübingen, Germany.

0012-821X/02/$ – see front matter
PII: S0012-821X(01)00584-2

1. Introduction

The behavior of volatiles in the Earth's mantle is crucial for the evolution of the Earth's atmosphere and hydrosphere, which were formed by degassing of the Earth's interior. This process involved the dissolution of volatiles in silicate melts at high pressures in the Earth's mantle, the ascent of the magma to the surface and subsequent exsolution of the dissolved gases and release towards the atmosphere. The increasing volatile solubility in silicate melts with pressure is experimentally well established for many different gases up to 3 GPa, corresponding to a depth of about 100 km (e.g. [3–6]), and it is assumed that this trend continues to much higher pressures. Among these volatiles are noble gases and because of their inert character and the existence of radiogenic isotopes, noble gases are widely used as tracers for studying mantle degassing and the evolution of the atmosphere (e.g. [7–9]).

Furthermore, data on noble gas solubility in silicate melts can be useful for understanding the solubility of more complex volatile species, such as H_2O, CO_2, CH_4, SO_2, which can also dissolve as neutral molecules in the melt. In this context, noble gas solubility is sometimes used as a probe for the interstitial melt structure, as it is thought that noble gases dissolve physically in the 'holes' or interstitial sites of the three-dimensional network of the melt [10–12], implying that the solubility depends on the available geometrical sites in the melt structure and their size distribution [13].

After studying Ar solubility in olivine and silica melt at very high pressures (up to 11 GPa) in a laser-heated diamond anvil cell (DAC) an unexpected effect was recently reported [1,2]. In these works an abrupt and drastic, one order of magnitude decrease of argon solubility was observed for both melt compositions at about 5 GPa, which was attributed to a compression of interstitial sites in the silicate melt making the melt incapable of accommodating noble gas atoms in its structure. If this interpretation is correct, it should also apply for all other noble gases or other physically dissolved molecules. A geochemical consequence of an extremely low noble gas solubility in melts would be that noble gases become moderately compatible or even compatible elements in the mantle at depths greater than 150 km, thus questioning the generally accepted view on how the Earth's atmosphere evolved [14]. On the other hand, more recent experiments on crystal/melt partitioning of noble gases found no change in (in)compatibility between 1 bar and 8 GPa [15], implying that magma transport to the surface is an efficient process for mantle degassing.

In this paper we present new experimental data on the solubility of argon and xenon in synthetic, Fe-free tholeiitic and haplogranitic melts up to 11 GPa. These systems are much closer in composition to natural melts than those studied previously by [1,2]. Tholeiite melts are commonly formed by partial melting in the upper mantle, while granitic melts may form by melting of subducted sedimentary rocks. In none of these systems do we observe any evidence of a drastic, abrupt decrease of noble gas solubility, even at pressures more than twice that of the previously reported solubility drop.

2. Experimental methods

2.1. Starting materials

The haplogranitic composition (HPG, $Qz_{39}Ab_{36}Or_{25}$ in wt%) was chosen for its relatively low melting temperature and its facility to quench to a glass. The three-dimensional silicate network of this melt is fully polymerized, similar to that of silica melt. Except for the presence of Al compensated by charge balancing cations, there is no fundamental difference from a melt structure point of view. Therefore, HPG can be used for testing the previous high pressure results for Ar solubility in silica melt [1]. The anhydrous HPG starting glass was melted from a mixture of reagent-grade Na_2CO_3, K_2CO_3, Al_2O_3, and SiO_2 at 1 atm and 1600°C for 1 h. After a first melting and quenching, the glass was ground and remelted in order to obtain a more homogeneous sample.

In order to study a melt composition more relevant to the Earth's mantle we used a synthetic, Fe-free tholeiite composition (THO), which pro-

Table 1
Compositions of the starting glasses in wt%

	HPG	THO
SiO_2	79.76	59.65
TiO_2	–	2.08
Al_2O_3	11.45	14.21
CaO	–	8.90
MgO	–	10.28
Na_2O	4.58	3.30
K_2O	4.21	1.58
Total	100.00	100.00

duces partially depolymerized melts. The starting glass was provided by M. Nowak, University of Hannover, and was also synthesized at 1600°C. The chemical composition is equivalent to a typical tholeiite melt [16], but in order to prevent iron loss toward the noble metal sample capsules during the experiments, iron oxide was replaced by MgO. However, for the general melt structure this exchange has no important consequences due to the similar roles of Mg^{2+} and Fe^{2+}. The chemical compositions of the starting glasses were determined by electron microprobe analysis and are given in Table 1.

2.2. Capsule preparation

Sample containers were Pt or $Pt_{95}Rh_5$ capsules with 3.5 mm length, 2.0 mm outer diameter and 0.2 mm wall thickness. Noble gases were loaded together with 2–3 mg glass powder into the sample capsules using a gas loading apparatus and procedures as described in [17] and were sealed by welding. Before putting the sample-containing capsule into the gas loading apparatus, the starting glass was dried together with the capsule at 500°C for 1 h, to remove surface water. Then the capsule was placed into the gas loading apparatus and was filled with the gas of interest. Subsequently, the gas was evacuated using a vacuum pump attached to the gas loading apparatus. Prior to welding, this process was repeated two or three times to purge the ambient atmosphere from the capsule in order to reduce contamination. Using this technique, 40–100 bar of the gas was loaded, resulting in 5–10 wt% Xe and 10–15 wt% Ar, which was always sufficient to saturate the entire sample.

2.3. High pressure experiments

For piston cylinder experiments the sample capsule was inserted into a mould of pressed MgO and sealed by welding into a second capsule (5 mm outer diameter, 10 mm length). This procedure allowed having two sample capsules in one experiment, but was also necessary as the gas-loaded sample capsules are much smaller than the capsules used in our piston cylinder apparatus. The double capsules were inserted into talc-pyrex or NaCl-pyrex cells (3/4 and 1/2 inch) with tapered graphite heaters. Experiments were brought to temperature after compression using the hot piston out technique as described in [18]. Temperatures were measured with S-type thermocouples, which were located at the top of the outer capsule. Pressure was calibrated against the quartz–coesite and kyanite–sillimanite transitions as well as the melting point of diopside (C.J.S. Shaw, personal communication). A friction correction of 18% for the talc-pyrex cells was applied to the nominal pressure on the basis of these calibrations. A friction correction of 10% was applied for NaCl-pyrex cells. Experiments were quenched after run durations of 30–120 min by switching off the furnace, while maintaining manually the sample pressure in order to compensate the pressure drop upon cooling. Temperatures dropped from 1500 to 400°C within 25 s.

Multi-anvil experiments were conducted in a 1200 t press as described in [19]. For the haplogranitic melts 25/17 and 18/11 type assemblies were used (edge lengths of the MgO octahedron/truncated edge lengths of the tungsten carbide anvils); all experiments with the THO composition were performed in 18/11 assemblies. For the larger 25/17 assembly, the 2 mm outer diameter sample capsule was inserted into a mould of pressed MgO and sealed by welding into a second capsule (4 mm outer diameter, 4 mm length). All other experiments (18/11 assemblies) were performed with single capsules. The sample capsule was placed in the center of a stepped $LaCrO_3$ furnace and was inserted into the MgO octahedron, which is used as the pressure transmitting medium. Each sample was first compressed at room temperature to the desired pressure and

was then heated at a rate of 100 or 200°C/min to superliquidus temperatures (1500–2000°C). The temperature was controlled using a D-type thermocouple, located at the top of the sample capsule. No correction for the effect of pressure on the thermocouple emf was made. The relationship between load and sample pressure at high temperature was calibrated at 1600 and 1800°C using the phase transformations of quartz–coesite and coesite–stishovite [20]. Experiments were terminated after run durations of 30–60 min by switching off the heater. The melts quenched to glasses within a few seconds. For the 25/17 and 18/11 assemblies the temperature dropped from 1800 to 400°C in about 11 and 5 s, respectively, with the fastest cooling rates at the beginning of the quench.

During the experiments, it is assumed that Ar or Xe was present in the sample capsule as a separate fluid phase and dissolved by diffusion into the melt phase until saturation was reached. After the experiments, the recovered sample capsules were opened by grinding on wet abrasive paper and in most cases some bubbling out of gas was observed. Finally sections from the sample centers were polished for further investigation.

2.4. Analytical techniques

The noble gas concentration in the glasses was determined by electron microprobe (Cameca SX 50). Analytical conditions for Ar and all other elements except Xe were 15 kV accelerating voltage, 15 nA beam current and a beam diameter of 10 μm. Xe was analyzed using 20 kV, 50 nA, 10 μm. Counting times were 30 s for Ar and Xe, and 20 s for all other elements. For Ar, a silica glass with known Ar content was used as standard (provided by K. Roselieb, labeled C&S in [21]). For electron microprobe analysis no Xe standard was available. This problem was overcome by preparing Xe-saturated albite glasses at 1.5 and 2.0 GPa and 1500°C, for which Xe solubility was reported previously [5]. Assuming that our albite glasses have the same Xe content as those of [5], our glasses were used as standards. Accordingly, the error in absolute concentration may be larger for Xe than for Ar, but this has no consequence for the relative evolution of the Xe solubility as a function of pressure.

3. Results and discussion

In general, the melts quenched to clear glasses containing few large bubbles (Fig. 1) but in two cases some crystals were also present. The presence of large bubbles indicates fluid saturation during the run. No microbubbles were detected by scanning electron microscopy (SEM), suggesting that no noble gas exsolution occurred upon quenching. The noble gas concentration in the glasses was determined by electron microprobe analysis. At least 10–25 points were analyzed in each glass and some glasses were repeatedly analyzed two or three times with similar results, thus demonstrating good analytical reproducibility. Elemental mapping of the samples with the electron microprobe demonstrated chemical homogeneity throughout the entire size of the sample (Fig. 1). The noble gas concentration close to bubbles or the capsule walls was identical to that of the specimen centers, suggesting that no gas diffused out of the samples during the quench. The homogeneity of the noble gas concentrations is also reflected by the low standard deviation of our analyses (Table 2).

Our data for Ar are shown in Fig. 2. For both haplogranitic and tholeiitic melt compositions we observe a similar evolution of the Ar solubility as a function of pressure. The Ar concentration increases linearly with pressure up to about 4–5 GPa, then it levels off and remains constant at higher pressures. The maximum solubility of Ar in the HPG melt is about 4.0 wt%, corresponding to 3.1 mol% calculated on the basis of 1 oxygen for the Ar-free silicate composition, or 1.4×10^{21} Ar atoms/cm^3 (based on a glass density of 2.32 g/cm^3). In our tholeiitic melt the Ar solubility reaches 0.8 wt%, which corresponds to 0.67 mol% or 3.1×10^{20} Ar atoms/cm^3 (based on a glass density of 2.60 g/cm^3). These differences in Ar solubility are consistent with the well-established dependence of noble gas solubility on the silicate melt composition. It was shown previously that noble gas solubility in silicate melts and

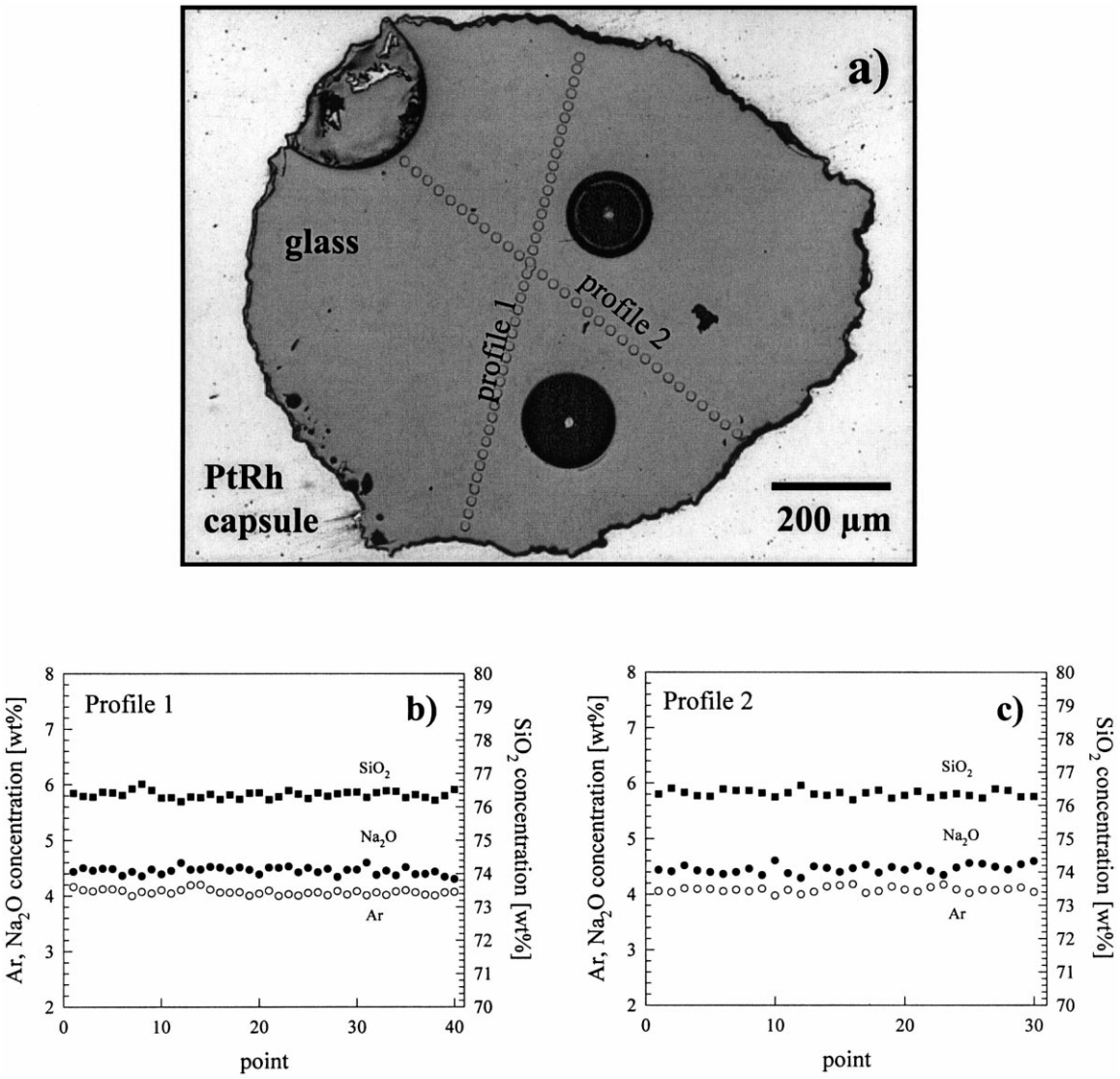

Fig. 1. (a) Photograph of a typical sample (BSA22, 7.4 GPa, 1900°C) prepared for electron microprobe analysis. The exposed and polished section was prepared from the central part of the sample. The gray area is the quenched glass, surrounded by the $Pt_{95}Rh_5$ capsule (light gray). Three large bubbles are exposed (one is filled with epoxy resin). No crystals or microbubbles were detected with SEM techniques. Profiles measured from rim to rim (b) or from bubble wall to rim (c) demonstrate chemical homogeneity throughout the entire sample. No Ar loss towards bubbles or the sample rim is observed.

glasses is highest for pure silica and decreases with increasing amount of network modifiers or substitution of Si by Al plus charge balancing cations [6,10–12,21]. This behavior suggests that noble gases dissolve in interstitial sites or 'holes' in the melt and glass structure and consequently the solubility was correlated with the ionic porosity, which is a measure for the interstitial space of the melt structure [11,12].

Experiments performed at a given pressure but at different temperatures show no systematic variation of the Ar concentration, suggesting negligible temperature dependence of Ar solubility. This is consistent with previously published low

Table 2
Conditions and results for Ar and Xe solubility experiments in haplogranitic and tholeiitic melts at high pressures

Sample	Apparatus	Assembly	*P* (GPa)	*T* (°C)	Duration (min)	Result	Ar/Xe (wt%)	Max. dev.	S.D.	Ar/Xe[a] (mol%)	S.D.[a]
HPG melt+Ar											
BSA15B	PC	NaCl-pyrex	1	1500	60	cg, lb	1.02	0.070	0.050	0.82	0.040
BSA8	PC	talc-pyrex	1	1600	30	cg, lb	1.09	0.130	0.081	0.88	0.066
BSA9	PC	talc-pyrex	1	1600	120	cg, lb	0.83	0.130	0.059	0.67	0.048
BSA29	PC	NaCl-pyrex	2	1500	60	cg, lb	2.08	0.130	0.059	1.68	0.048
BSA11	PC	talc-pyrex	2	1600	90	cg, lb	2.04	0.090	0.038	1.65	0.031
BSA27	MA	18/11	2.2	1600	60	cg, lb	1.66	0.080	0.051	1.34	0.041
BSA21	MA	25/17	2.25	1600	60	cg, lb	1.85	0.090	0.053	1.50	0.043
BSA25	MA	18/11	2.85	1600	60	cg, lb	2.44	0.090	0.042	1.98	0.034
BSA12	PC	talc-pyrex	3	1600	30	cg, lb	2.97	0.100	0.062	2.41	0.051
BSA19	MA	25/17	3	1600	60	cg, lb	2.74	0.060	0.038	2.22	0.031
BSA18	MA	25/17	3	1800	10	cg, lb	2.58	0.120	0.078	2.09	0.064
BSA15	MA	25/17	3.75	1800	60	cg, lb	2.97	0.170	0.068	2.41	0.055
BSA28	MA	18/11	3.8	1600	60	cg, lb	3.26	0.130	0.063	2.64	0.051
BSA14	MA	25/17	4.125	1800	60	cg, lb	3.39	0.110	0.067	2.75	0.055
BSA20	MA	25/17	4.5	1800	60	cg, lb	3.59	0.100	0.062	2.91	0.051
BSA17	MA	25/17	5.25	1800	60	cg, lb	3.94	0.080	0.044	3.20	0.036
BSA7	MA	25/17	6	1800	60	cg, lb, co	3.94	0.070	0.045	3.20	0.037
BSA22	MA	18/11	7.4	1900	30	cg, lb	4.06	0.100	0.049	3.30	0.040
BSA23	MA	18/11	8.2	1950	30	cg, lb, co	3.95	0.180	0.104	3.21	0.085
THO melt+Ar											
THO17	PC	NaCl-pyrex	1	1500	60	cg, lb	0.25	0.030	0.018	0.21	0.015
THO7	PC	NaCl-pyrex	2	1500	60	cg, lb	0.45	0.050	0.028	0.38	0.024
THO10	MA	18/11	2.2	1600	60	cg, lb	0.39	0.030	0.015	0.33	0.013
THO6	MA	18/11	2.85	1600	60	cg, lb	0.52	0.030	0.018	0.44	0.015
THO16	PC	NaCl-pyrex	3	1500	60	mg, lb	0.66	0.120	0.071	0.56	0.061
THO8	MA	18/11	3.8	1800	60	cg, lb	0.71	0.050	0.032	0.61	0.027
THO5	MA	18/11	4.85	1800	60	cg, lb	0.76	0.050	0.035	0.65	0.030
THO15	MA	18/11	5.55	1800	60	cg, lb	0.74	0.050	0.025	0.63	0.021
THO2	MA	18/11	6.4	1900	60	cg, lb	0.81	0.040	0.021	0.69	0.018
THO21	MA	18/11	7.1	1900	60	cg, lb	0.78	0.040	0.020	0.66	0.017
THO14	MA	18/11	8.2	2000	45	cg, lb	0.80	0.090	0.036	0.68	0.031
THO19	MA	18/11	9.7	2000	30	cg, lb	0.81	0.050	0.031	0.69	0.026
THO melt+Xe											
THOX10	PC	NaCl-pyrex	1.5	1500	60	cg, lb	0.32	0.030	0.013	0.08	0.003
THOX4	PC	NaCl-pyrex	2	1500	60	cg, lb	0.41	0.020	0.012	0.11	0.003
THOX8	MA	18/11	3.5	1600	60	cg, lb	0.57	0.040	0.019	0.15	0.005
THOX6	MA	18/11	5	1800	60	cg, lb	0.76	0.030	0.018	0.20	0.005
THOX3	MA	18/11	7	1900	60	cg, lb	0.84	0.030	0.018	0.22	0.005
THOX7	MA	18/11	9	2000	30	cg, lb	0.81	0.040	0.015	0.21	0.004
THOX1	MA	18/11	11	2000	30	cg, lb	0.80	0.030	0.016	0.21	0.004

PC: piston cylinder; MA: multi-anvil; cg: clear glass; mg: milky glass; lb: large bubbles present; co: coesite present.
[a] mol% calculated on the basis of 1 oxygen for the noble gas-free silicate composition.

pressure data for similar melt compositions [5,6,11,22]. We observe no abrupt and drastic drop in argon solubility either for the haplogranitic or for the tholeiitic composition, even at pressures near 10 GPa, twice the pressure of the solubility drop reported by [1,2]. If the solubility drop observed in these studies were due to a reduction of the size of interstitial cavities in the melt, it should occur at even lower pressures for a noble gas with a higher atomic radius than Ar. Accordingly, we performed similar experiments with the heaviest stable noble gas, Xe. The Xe

solubility exhibits a pattern very similar to that of Ar (Fig. 3). First, the Xe solubility increases linearly with pressure up to about 6 GPa where it reaches 0.8 wt% (corresponding to 0.21 mol%, calculated on the basis of 1 oxygen for the Ar-free silicate composition or 9.5×10^{19} Xe atoms/cm^3), then the solubility remains constant at least up to 11 GPa. Following the model proposed by [2], a drop in Xe solubility would be expected to occur near 2 GPa. Our data in Fig. 3 show no such effect up to 11 GPa. This suggests that for a relatively small noble gas such as Ar, a drop in solubility due to changes in hole size distribution is not even to be expected at pressures far beyond the pressure range we studied experimentally and which covers nearly the entire upper mantle.

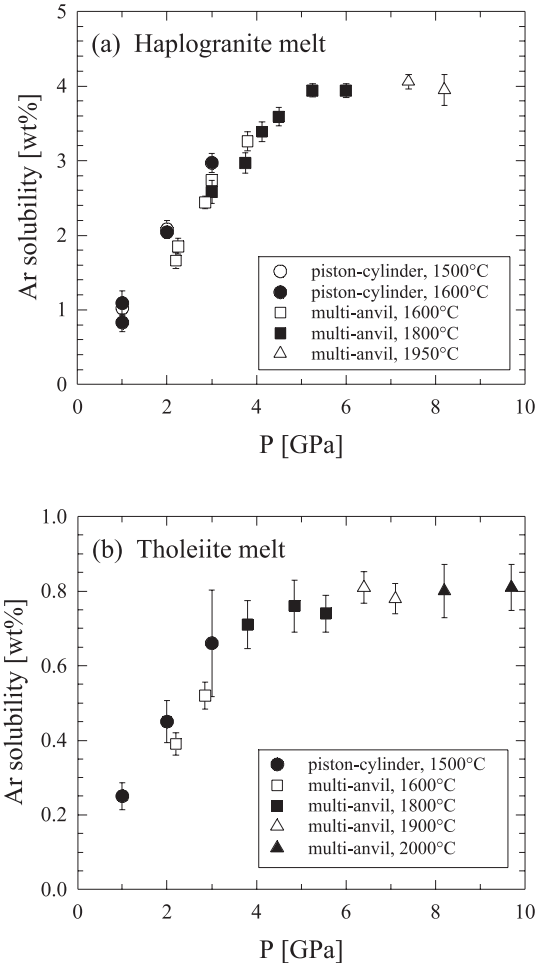

Fig. 2. Ar solubility (in wt%) in haplogranitic (a) and tholeiitic melts (b) as a function of pressure. Error bars correspond to 2σ of the microprobe analysis.

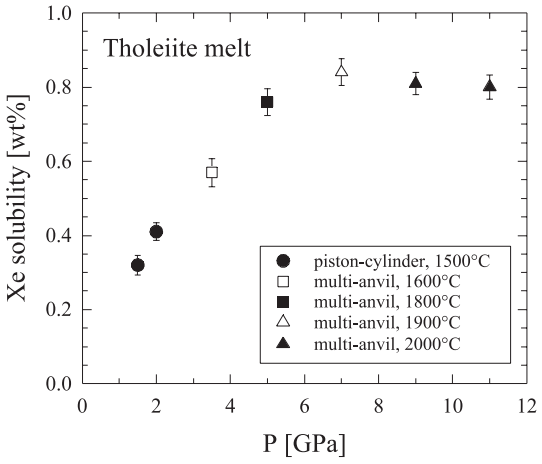

Fig. 3. Xe solubility (in wt%) in tholeiitic melt as a function of pressure. Error bars correspond to 2σ of the microprobe analysis.

The silicate melts studied here differ in compositions from those investigated by [1,2]. One may therefore suspect that the compositional differences may be responsible for the different pressure effect of noble gas solubility of these studies. This is, however, rather unlikely, as in both studies two very different melt compositions were investigated, ranging from completely polymerized haplogranitic or silica melts to depolymerized tholeiite or olivine melts. It was noted in [1,2] that the silica melt partially crystallized upon quenching and the authors discussed the possibility that the apparent drop in argon solubility may be due to exsolution during quenching. In the case of olivine melt, Raman spectra also indicated the presence of some quench crystallization. In contrast to this, no evidence for quench crystallization or diffusional loss of noble gases was observed in the present study. A potential problem for studying Ar solubility in silicate melts at high pressures using a laser heated DAC is the extremely small sample volume, which may allow diffusional loss of Ar during quenching. Such effects may occur upon partial crystallization as it was reported in the work of [1,2]. In our study, we avoided this problem by using a multi-anvil apparatus, which allows not only a much larger sample volume

(about three orders of magnitude larger than that of a DAC), but also a better control of pressure and temperature. Moreover, the melts investigated in the present study were not subject to any quench crystallization.

In this study we determined maximum noble gas solubility in silicate melts, which means that the melts were in equilibrium with pure noble gases (noble gas activity = 1). However, noble gas concentrations in the Earth's mantle are several orders of magnitude lower than in our experiments. Therefore, it may be questioned whether our results are actually applicable to mantle conditions. This problem may be addressed by comparing the results of the present study with data obtained from noble gas mass spectrometry for melts equilibrated with noble gases at low partial pressures (e.g. [23–27]). In these studies noble gas concentrations were expressed as *cm^3 STP/g bar*, where 1/bar means 'per bar partial pressure of loaded gas' and which corresponds to Henry's law constant. For the present data for Ar in THO melt we can calculate: 0.8 wt% Ar corresponds to 3.1×10^{20} atoms/cm^3 (based on a glass density of 2.60 g/cm^3) = 5.15×10^{-4} mol/cm^3 = 11.54 cm^3 STP/cm^3 = 4.44 cm^3 STP/g. At an Ar partial pressure of 5 GPa this corresponds to 8.88×10^{-5} cm^3 STP/g bar. This value can be compared with Henry's law constants derived from mass spectrometry data for basaltic melts (e.g. Broadhurst et al. [23], $1–17\times10^{-5}$ cm^3 STP/g bar, pressure: 1 bar; Hiyagon and Ozima [24], $2–4\times10^{-5}$ cm^3 STP/g bar, pressure: 1 bar; Lux [25], $6–12\times10^{-5}$ cm^3 STP/g bar, pressure: 1 bar; Jambon et al. [26] $5–8\times10^{-5}$ cm^3 STP/g bar, pressure: 1 bar; Shibata et al. [27], $9–23\times10^{-5}$ cm^3 STP/g bar, pressure range: 500–2000 bar). Considering the differences in melt composition, this comparison shows that Henry's law constants obtained from very different pressure and concentration regimes are in relatively good agreement, suggesting similar incorporation mechanisms. For Xe in THO melt a Henry's law constant of 2.59×10^{-5} cm^3 STP/g bar can be derived from our data (e.g. 0.76 wt% Xe = 9.06×10^{20} atoms/cm^3 at 5 GPa), which also agrees well with previous low pressure data for basalt melts ranging between 0.3 and 3.6×10^{-5} cm^3 STP/g bar [23–26]. Accordingly, we believe that our data can be safely extrapolated to much lower partial pressures of noble gases.

Our experimental data show that noble gas solubilities in silicate melts at mantle pressures remain high and do not drop by an order of magnitude as suggested by [1,2]. Therefore it can be expected that the observed solubilities in the silicate melts are orders of magnitude higher than noble gas solubilities in mantle minerals. This would mean that noble gases remain incompatible elements at least within the entire upper mantle and that partial melting is extremely efficient in extracting noble gases and other volatiles out of the Earth's mantle. This conclusion is consistent with recent determinations of noble gas crystal/melt partition coefficients using micro-analytical techniques [15,28,29] rather than bulk measurements (e.g. [23,24,30,31]).

Roselieb et al. [28] studied Ar sorption in quartz at 1300°C and pressures up to 8 kbar. Using different analytical techniques like gas chromatography (GC), Knudsen cell mass spectrometry (KMS), electron microprobe, and SEM these authors measured Ar concentrations ranging from a few tens to several thousands ppm for a given sample. It was concluded that this variation is probably caused by Ar trapped in gas inclusions and/or Ar adsorbed in fractures or other planar defects. Because such Ar atoms cannot be discriminated from truly dissolved Ar with bulk analytical methods like GC or KMS, bulk measurements will not document equilibrium dissolution but will yield variable Ar concentrations, which depend on experimental conditions and significantly overestimate the true solubility. Such effects may indeed account for the large variation of noble gas crystal melt partition coefficients available in the literature (e.g. [23,24,27,30,31]), which for Ar scatters over more than two orders of magnitude. Based on the statistics of their EMP data [28] derived a quartz/melt partition coefficient for Ar of less than 0.006, Brooker et al. [29] and Chamorro et al. [15] determined Ar and Kr partition coefficients for olivine and clinopyroxene grown from silicate melts by using an ultraviolet laser ablation microprobe technique, which enables measurements of noble gas concen-

trations in individual crystals as well as in glasses. Whereas [29] performed experiments at 1 bar Ar pressure, [15] conducted experiments at pressures up to 8 GPa but low noble gas concentrations. For both studies, the derived partition coefficients are several orders of magnitude lower than those of previous measurements on separated crystal–glass pairs. Brooker et al. [29] and Chamorro et al. [15] argue that higher values for crystal/melt partition coefficients may result from melt inclusions or other heterogeneous distributions of 'non-equilibrium' noble gases in crystals.

In the past, two alternative thermodynamic models were employed to describe the pressure effect on noble gas solubility in silicate melts. Both models were able to fit the available data up to 3 GPa with equal success and it was assumed that data at higher pressures were necessary in order to distinguish between the two models [10,21]. Solubility data for Ar and Xe are now available for pressures up to 11 GPa and a leveling off in noble gas solubility can be observed. Indeed a leveling off in noble gas solubility at high pressures may imply that the interstitial sites in the melt structure, suitable for the accommodation of noble gas atoms, are fully occupied. In this model, the observed variation of the 'leveling off pressure' (HPG-Ar: 5 GPa, THO-Ar: 4 GPa, THO-Xe: 6 GPa, Figs. 2 and 3) may indicate that for different melt compositions and noble gases, complete filling is achieved at different pressures, which is reasonable to assume. However, in the light of the experimental error of multi-anvil experiments (at least 0.5 GPa), it is impossible to decide whether these variations are representative for the different systems or not. It is also surprising that the 'leveling off pressure' for a given silicate melt composition (here THO) seems to be higher for Xe than for Ar. It may intuitively be expected that for the large noble gases, for which fewer suitable sites are available, complete filling is achieved at lower pressures. On the other hand, the result may simply suggest that it is more difficult for Xe to 'find' suitable sites than it is for smaller noble gases. However, in the next section we will demonstrate that a thermodynamic mixing model is also capable of reproducing the experimental data without assuming any fixed population of interstitial sites. Moreover, we will show that it is virtually impossible to decide which model is more appropriate for the description of the pressure effect on noble gas solubility in silicate melts.

3.1. Model assuming mixing of argon atoms and oxygen atoms in the melt

The first model treats the melt as a mixture of the noble gas atoms with the oxygen atoms of the silicate matrix. If the activity coefficients of the noble gas atoms in the melt are assumed to be constant, this model can be described by the equation:

$$\ln\left(\frac{X_{NG}\cdot f^{\circ}_{NG}}{X^{\circ}_{NG}\cdot f_{NG}}\right) = -\left(\frac{\Delta H^{\circ}_{NG}}{R}\right)\cdot\left(\frac{1}{T}-\frac{1}{T^{\circ}}\right)-\left(\frac{V^{\circ}_{NG}}{RT}\right)\cdot(P-P^{\circ}) \quad (1)$$

where X_{NG} is the molar fraction of the noble gas in the melt, f_{NG} is the noble gas fugacity in the vapor phase, the superscript ° refers to a reference state which can be arbitrarily chosen, ΔH°_{NG} is the molar enthalpy of solution of the noble gas at the reference pressure and temperature, V°_{NG} is the standard state molar volume of the noble gas in the melt and R is the gas constant. Eq. 1 assumes that V°_{NG} is independent of P and T, and that ΔH°_{NG} is independent of T. A more detailed description of the assumptions and derivations for this model is given in [10]. Noble gas fugacities at P and T were calculated using a modified Redlich–Kwong equation of state [32,33], using data for the corresponding states parameters of Ar and Xe (Ar: $T_{crit}=150.9$ K, $P_{crit}=4.898$ MPa; Xe: $T_{crit}=289.7$ K, $P_{crit}=5.84$ MPa) from [34]. In the isothermal case, Eq. 1 reduces to:

$$X_{NG} = \frac{X^{\circ}_{NG}\cdot f_{NG}}{f^{\circ}_{NG}}\cdot\exp\left(-\frac{V^{\circ}_{NG}\cdot(P-P^{\circ})}{R\cdot T}\right) \quad (2)$$

For technical reasons we were not able to perform isothermal noble gas solubility experiments over the entire pressure range of 1–11 GPa and our data sets display a temperature variation of

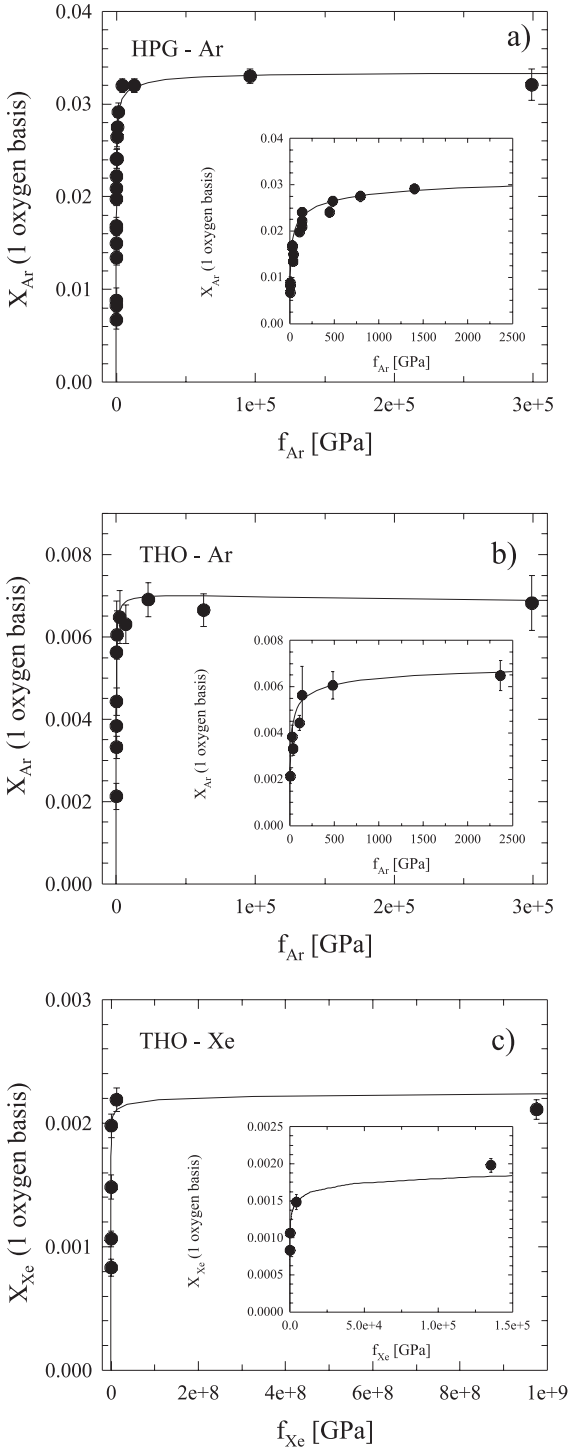

Fig. 4. Noble gas solubility in the systems HPG-Ar (a), THO-Ar (b) and THO-Xe (c) as a function of gas fugacity. Noble gas fugacities were calculated for 1800°C, assuming a negligible effect of temperature on the noble gas solubility in these systems (see text for details). Molar fractions were calculated on the basis of 1 oxygen for the noble gas-free silicate composition. Symbols indicate experimental data, error bars correspond to 2σ of the microprobe analysis and the solid lines are the fits of Eq. 2 to the data. Insets show enlargements for the first data points.

→

500°C (1500–2000°C, Table 2). However, it was shown in previous studies [5,6,22], and it also appears from this work, that a possible effect of temperature on noble gas solubility is smaller than the experimental error. Therefore, we assumed that the temperature effect on noble gas solubility can be neglected, and we calculated the noble gas fugacities for the thermodynamic modeling for a constant temperature of 1800°C. The fits of our experimental data with Eq. 2 are shown in Fig. 4. The reference state was arbitrarily chosen to be 1800°C and 3.8 GPa for the systems HPG-Ar and THO-Ar, and 1800°C and 3.5 GPa for THO-Xe. The molar fraction of the dissolved noble gases in the quenched melts was calculated on the basis of 1 oxygen for the noble gas-free silicate composition. It is obvious that this model is capable of successfully reproducing the experimental data for all systems studied (Fig. 4). The results for $V°_{NG}$ obtained from the fits are listed in Table 3. The values for $V°_{Ar}$ in HPG and THO are nearly identical and compare very well with the $V°_{Ar}$ data for granitic (23.1 cm^3/mol) and olivine tholeiitic (23.7 cm^3/mol) melts of [6]. The similarity of $V°_{Ar}$ in HPG and THO melts may suggest that the Ar atoms occupy sites with similar geometry, despite the fact that the melt structures of HPG and THO are quite different (HPG fully polymerized, THO partly depolymerized). Our value for $V°_{Xe}$ in THO (37.4 cm^3/mol) is significantly higher than the values of $V°_{Xe}$ reported by [5] for feldspathic and $K_2Si_4O_9$ melts (28.0–29.4 cm^3/mol). We do not know the reason for this discrepancy; however, our values of partial molar volumes for both Ar and Xe are close to the *b*-parameter in the Redlich–Kwong equation (Table 3). This parameter is a rough measure for

the atomic volume and was suggested to provide an approximation to the partial molar volumes of molecular gas species in silicate melts [11].

From a thermodynamic point of view, the constant noble gas solubility at high pressures simply implies that the partial molar volumes of the respective noble gas in the fluid and in the melt are equal. Indeed, the molar volumes of Ar and Xe in the fluid phase calculated with the Redlich–Kwong equation of state [32,33] approach values, which at 5 GPa, 1800°C, are only 5% higher than the respective molar volumes in the quenched melts. Since noble gases do not chemically interact with their matrix, it is reasonable to assume that in highly compressed liquids their partial molar volumes are identical. Following this line of reasoning a sudden change in solubility at higher pressures is not to be expected.

3.2. Fixed population of holes

The second model treats the noble gas solubility as a homogeneous solution of the noble gas atoms into a fixed population of holes. It requires that the number of available sites is independent of pressure, temperature and number of dissolved atoms. In assuming that the volume of such holes (or interstitial sites) remains unchanged upon filling, i.e. that there is no effect of the solute on solvent structure, the solubility can be described by the Langmuir adsorption isotherm:

$$k_L = n/(M-n)f \quad (3)$$

where k_L is the equilibrium constant, n is the number of dissolved atoms, M is the number of available sites and f is the fugacity. A more detailed description of the assumptions and derivations for this model can be found in [10]. Fig. 5 shows the fit of the experimental data with the Langmuir isotherm. In contrast to previous studies [10,21,22], the constant M (representing the number of available sites in the melt) was not assumed, but was obtained directly from the threshold solubility where the dissolved noble gas concentration levels off. The obtained parameters k_L and M are listed in Table 3. The number of available sites for Ar in HPG is about four times higher than in THO, representing significant structural differences. HPG has a fully polymerized structure, which in analogy to quartz–feldspar glasses may be described in a first approximation by the stuffed tridymite-like structure [35]. This structure consists of a three-dimensional network of six-membered (alumino)silicate rings in which some of the interstitial sites are occupied by Na and K, which charge compensate Al in tetrahedral coordination. For our HPG composition this model would leave more than 60% of the interstitial sites unoccupied of which suitable sites may be filled with Ar (or other noble gases). In contrast to HPG, the tholeiitic melt has a depolymerized structure with a NBO/T of 0.53 (NBO/T = non-bridging oxygen per tetrahedron). Such structure is more compact and has fewer suitable interstitial sites or ring units available for the accommodation of Ar (or other noble gases). It should be mentioned that our values of M for Ar in HPG and THO are two to four times higher than those in previous studies for comparable melt compositions [10,21,22]. The reason for this discrepancy is that in previous studies M was an adjustable parameter of the fit. Since solubility data were only available for lower pressures

Table 3
Best fit parameters for Eqs. 2 and 3

	$V°$ (cm^3/mol)	b-parameter MRK (cm^3/mol)	M[c] (10^{20} sites/cm^3 melt)	k_L (10^{-6} bar^{-1})
HPG-Ar[a]	24.3 ± 0.2	22.21	13.8 ± 0.3	1.1 ± 0.2
THO-Ar[a]	24.7 ± 0.3	22.21	3.10 ± 0.15	2.5 ± 0.5
THO-Xe[b]	37.4 ± 0.3	35.76	0.96 ± 0.03	0.1 ± 0.03

[a] Reference state: 3.8 GPa, 1800°C.
[b] Reference state: 3.5 GPa, 1800°C.
[c] The number of sites was directly taken from the experimentally determined threshold concentration.

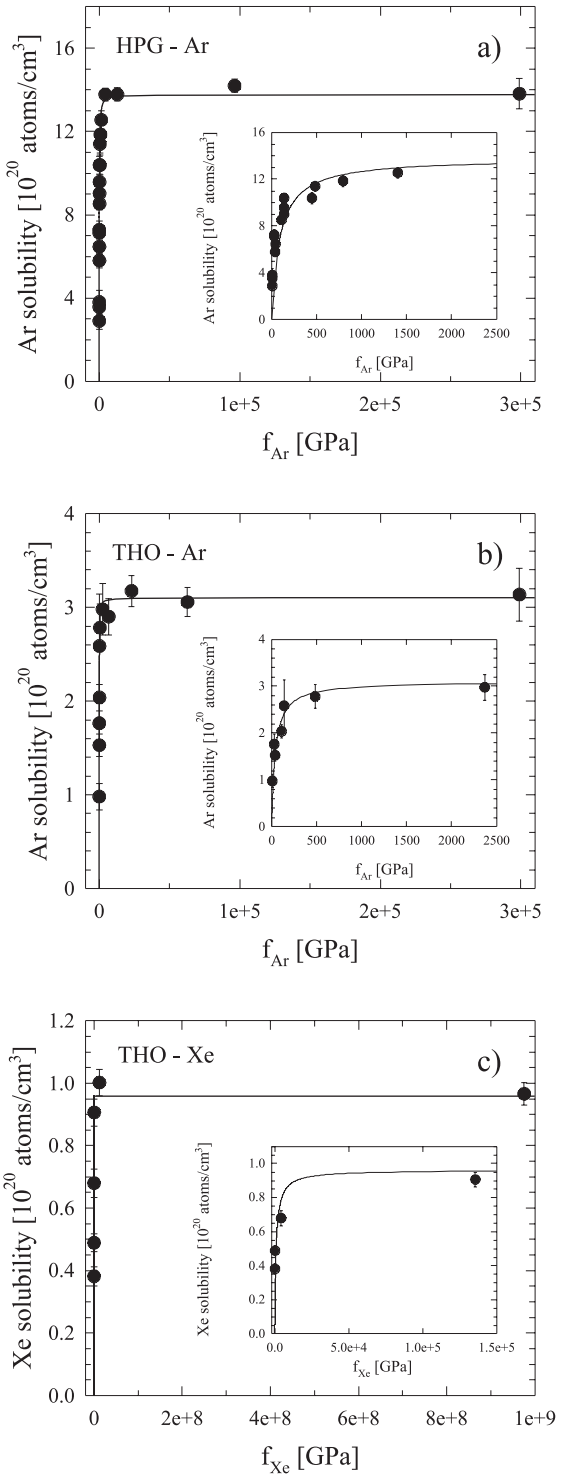

Fig. 5. Noble gas solubility (in atoms/cm^3) in the systems HPG-Ar (a), THO-Ar (b) and THO-Xe (c) as a function of gas fugacity. Noble gas fugacities were calculated for 1800°C, assuming a negligible effect of temperature on the noble gas solubility in these systems (see text for details). Symbols indicate experimental data, error bars correspond to 2σ of the microprobe analysis and the solid lines are the fits of Eq. 3 (Langmuir isotherm) to the data. Insets show enlargements for the first data points.
←

(<2.5 GPa) the leveling off of the noble gas solubility was not observed and M was estimated to smaller numbers than what we find experimentally. As a consequence of the low M values, the numbers for k_L are two orders of magnitude higher than those determined in this study. Although the 'fixed population of holes' model (including all assumptions involved and its description with a Langmuir isotherm) is very simplistic, it is capable of fitting the observed argon and xenon solubility in haplogranitic and tholeiitic melts including the leveling off in noble gas solubility at high pressures. The latter effect may be interpreted as indicating complete filling of interstitial sites in the melt. However, it is questionable whether a model with defined, rigid sites is actually appropriate for a silicate melt, as high temperature ^{29}Si NMR data demonstrate fast exchange between silicon and oxygen atoms on the timescale of microseconds (or nanoseconds) in such melts [36,37]. Furthermore, X-ray absorption spectroscopy data suggest that Kr dissolved in silica glass has a very specific coordination geometry, closely surrounded by oxygen atoms [38], thus questioning the assumption that there is no effect of the dissolved noble gas on the silicate network.

4. Conclusions

Our study shows that it is possible to perform gas solubility experiments in a multi-anvil apparatus. We demonstrate that Ar and Xe solubility in haplogranitic and tholeiitic melts increases linearly with pressure up to a threshold concentration where the content of dissolved noble gas levels off. Although such a solubility pattern

intuitively suggests that noble gases dissolve into a fixed population of holes, a second thermodynamic model, which describes the solubility as a mixing of the noble gas atoms with the oxygen atoms of the silicate lattice, fits the data equally well. The results are in strong contrast with those of [1,2], who observed a drastic decrease of Ar solubility above 5 GPa. The geochemical implication of our results is that noble gases remain incompatible elements at pressures covering most of the upper mantle. Thus, partial melting is a highly efficient mechanism for mantle degassing. As a consequence, current models of mantle degassing and evolution of the atmosphere do not need to be reconsidered as was suggested by [1,2].

Acknowledgements

H.K. acknowledges support by the German Science Foundation (DFG). B.C.S. acknowledges funding by the 'visitors program' of the Bayerisches Geoinstitut. We thank Marcus Nowak for providing the THO glass and Knut Roselieb for providing the Ar standard. Detlef Krauße is thanked for assistance with the microprobe analysis. Jon Blundy, Mario Trieloff, and an anonymous reviewer improved the manuscript with helpful comments and suggestions. *[AH]*

References

[1] E. Chamorro-Perez, P. Gillet, A. Jambon, Argon solubility in silicate melts at very high pressures: Experimental set-up and preliminary results for silica and anorthite melts, Earth Planet. Sci. Lett. 145 (1996) 97–107.

[2] E. Chamorro-Perez, P. Gillet, A. Jambon, J. Badro, P. McMillan, Low argon solubility in silicate melts at high pressure, Nature 393 (1998) 352–355.

[3] J.G. Blank, R.A. Brooker, Experimental studies of carbon dioxide in silicate melts: Solubility, speciation, and stable isotope behaviour, in: M.R. Carroll, J.R. Holloway (Eds.), Volatiles in Magmas (Rev. Mineral. 30), Mineral. Soc. Am., Washington, DC, 1994, pp. 157–186.

[4] M.R. Carroll, J.D. Webster, Solubilities of sulfur, noble gases, nitrogen, chlorine, and fluorine in magmas, in: M.R. Carroll, J.R. Holloway (Eds.), Volatiles in Magmas (Rev. Mineral. 30), Mineral. Soc. Am., Washington, DC, 1994, pp. 231–279.

[5] A. Montana, Q. Guo, S.L. Boettcher, B.S. White, M. Brearley, Xe and Ar in high-pressure silicate liquids, Am. Mineral. 78 (1993) 1135–1142.

[6] B.S. White, M. Brearley, A. Montana, Solubility of argon in silicate liquids at high pressures, Am. Mineral. 74 (1989) 513–529.

[7] C.J. Allègre, T. Staudacher, P. Sarda, Rare gas systematics: formation of the atmosphere, evolution and structure of the Earth's mantle, Earth Planet. Sci. Lett. 81 (1986) 127–150.

[8] A. Jambon, Earth degassing and large-scale geochemical cycling of volatile elements, in: M.R. Carroll, J.R. Holloway (Eds.), Volatiles in Magmas (Rev. Mineral. 30), Mineral. Soc. Am., Washington, DC, 1994, pp. 479–517.

[9] M. Ozima, K. Zahnle, Mantle degassing and atmosphere evolution – noble gas view, Geochem. J. 27 (1993) 185–200.

[10] M.R. Carroll, E.M. Stolper, Argon solubility and diffusion in silica glass: Implications for the solution behavior of molecular gases, Geochim. Cosmochim. Acta 55 (1991) 211–225.

[11] M.R. Carroll, E.M. Stolper, Noble gas solubilities in silicate melts and glasses: New experimental results for argon and the relationship between solubility and ionic porosity, Geochim. Cosmochim. Acta 57 (1993) 5039–5051.

[12] T. Shibata, E. Takahashi, J.-I. Matsuda, Solubility of neon, argon, krypton and xenon in binary and ternary silicate systems: A new view on noble gas solubility, Geochim. Cosmochim. Acta 62 (1998) 1241–1253.

[13] J.F. Shackelford, A gas probe analysis of structure in bulk and surface layers of vitreous silica, J. Non-Cryst. Solids 49 (1982) 299–307.

[14] M. Ozima, Noble gases under pressure in the mantle, Nature 393 (1998) 303–304.

[15] E.M. Chamorro, R.A. Brooker, J.-A. Wartho, B.J. Wood, S.P. Kelley, J.D. Blundy, Ar and K partitioning between clinopyroxene-silicate to 8 GPa, Geochim. Cosmochim. Acta (2002) in press.

[16] T.N. Irvine, W.R.A. Baragar, A guide to the chemical classification of the common volcanic rocks, Can. J. Earth Sci. 8 (1971) 523–548.

[17] S.L. Boettcher, Q. Guo, A. Montana, A simple device for loading gases in high-pressure experiments, Am. Mineral. 74 (1989) 1383–1384.

[18] W. Johannes, P.M. Bell, H.K. Mao, A.L. Boettcher, D.W. Chipman, J.F. Hays, R.C. Newton, F. Seifert, An interlaboratory comparison of piston-cylinder pressure calibration using the albite-breakdown reaction, Contrib. Mineral. Petrol. 32 (1971) 24–38.

[19] D.C. Rubie, Characterising the sample environment in multianvil high-pressure experiments, Phase Trans. 68 (1999) 431–451.

[20] N.D. Chatterjee, R. Krüger, G. Haller, W. Olbricht, The Bayesian approach to an internally consistent thermodynamic database: theory, database, and generation of phase diagrams, Contrib. Mineral. Petrol. 133 (1998) 149–168.

[21] H. Walter, K. Roselieb, H. Büttner, M. Rosenhauer, Pressure dependence of the solubility of Ar and Kr in melts of the system SiO_2-$NaAlSi_2O_6$, Am. Mineral. 85 (2000) 1117–1127.
[22] K. Roselieb, W. Rammensee, H. Büttner, M. Rosenhauer, Solubility and diffusion of noble gases in vitreous albite, Chem. Geol. 96 (1992) 241–266.
[23] C.L. Broadhurst, M.J. Drake, B.E. Hagee, T.J. Bernatowicz, Solubility and partitioning of Ne, Ar, Kr, and Xe in minerals and synthetic basaltic melts, Geochim. Cosmochim. Acta 54 (1992) 709–723.
[24] H. Hiyagon, M. Ozima, Partition of noble gases between olivine and basalt melt, Geochim. Cosmochim. Acta 50 (1986) 2045–2057.
[25] G. Lux, The behavior of noble gases in silicate liquids: Solution, diffusion, bubbles and surface effects, with applications to natural samples, Geochim. Cosmochim. Acta 51 (1987) 1549–1560.
[26] A. Jambon, H. Weber, O. Braun, Solubility of He, Ne, Ar, Kr and Xe in a basaltic melt in the range 1250–1600°C Geochemical implications, Geochim. Cosmochim. Acta 50 (1986) 401–408.
[27] T. Shibata, E. Takahashi, M. Ozima, Noble gas partitioning between basaltic melt and olivine crystals at high pressures, in: J.I. Matsuda (Ed.), Noble Gas Geochemistry and Cosmochemistry, Terra Science Publishing, Tokyo, 1994, pp. 343–354.
[28] K. Roselieb, P. Blanc, H. Büttner, A. Jambon, W. Rammensee, M. Rosenhauer, D. Vielzeuf, H. Walter, Experimental study of argon sorption in quartz: Evidence for argon incompatibility, Geochim. Cosmochim. Acta 61 (1997) 533–542.
[29] R.A. Brooker, J.-A. Wartho, M.R. Carroll, S.P. Kelley, D.S. Draper, Preliminary UVLAMP determinations of argon partition coefficients for olivine and clinopyroxene grown from silicate melts, Chem. Geol. 147 (1998) 185–200.
[30] H. Hiyagon, M. Ozima, Noble gas distribution between basalt melt and crystals, Earth Planet. Sci. Lett. 58 (1982) 255–264.
[31] C.L. Broadhurst, M.J. Drake, B.E. Hagee, T.J. Bernatowicz, Solubility and partitioning of Ar in anorthite, diopside, forsterite, spinel, and synthetic basaltic liquids, Geochim. Cosmochim. Acta 54 (1990) 299–309.
[32] O. Redlich, J.N.S. Kwong, On the thermodynamics of solutions V. An equation of state. Fugacities of gaseous solutions, Chem. Rev. 44 (1949) 233–244.
[33] J.R. Holloway, Fugacity and activity of molecular species in supercritical fluids, in: D.G. Fraser (Ed.), Thermodynamics in Geology, Reidel, Dordrecht, 1977, pp. 161–181.
[34] D. Ambrose, Critical constants, boiling points, and melting points of selected compounds, in: D.R. Lide (Ed.), CRC Handbook of Chemistry and Physics, CRC Press, Boca Raton, FL, 1991, pp. 6-49–6-63.
[35] M. Taylor, G.E. Brown Jr., Structure of mineral glasses – I. The feldspar glasses $NaAlSi_3O_8$, $KAlSi_3O_8$, $CaAl_2Si_2O_8$, Geochim. Cosmochim. Acta 43 (1979) 61–75.
[36] I. Farnan, J.F. Stebbins, The nature of the glass transition in a silica-rich oxide melt, Science 265 (1994) 1206–1209.
[37] J.F. Stebbins, J.B. Murdoch, E. Schneider, I.S.E. Carmichael, A. Pines, A high-temperature high-resolution NMR study of ^{23}Na ^{27}Al and ^{29}Si in molten silicates, Nature 314 (1985) 250–252.
[38] R. Wulf, G. Calas, A. Ramos, H. Büttner, K. Roselieb, M. Rosenhauer, Structural environment of krypton dissolved invitreous silica, Am. Mineral. 84 (1999) 1461–1463.